DOI: 10.1021/ma901415h

Macromolecules
ARTICLE

Synthesis and Micellization of Linear−Dendritic Copolymers and Their Solubilization Ability for Poorly Water-Soluble Drugs

Zhengyuan Zhou,*,† Antony D'Emanuele,† Kieran Lennon,§ and David Attwood‡

†*School of Pharmacy and Pharmaceutical Sciences, University of Central Lancashire, Preston PR1 2HE, U.K.,* ‡*School of Pharmacy and Pharmaceutical Sciences, University of Manchester, Manchester M13 9PL, U.K., and* §*AstraZeneca, Pharmaceutical & Analytical R&D, Macclesfield, Cheshire SK10 2NA, U.K.*

Received July 1, 2009; Revised Manuscript Received August 11, 2009

ABSTRACT: A series of linear−dendritic copolymers were synthesized by conjugating BE block copolymers (B_8E_{41} and $B_{16}E_{42}$, B = 1,2-butylene oxide and E = ethylene oxide) with G1−3 PAMAM dendrimers via carbamate bonds. The critical micelle concentrations of the dendrimer conjugates were less than 0.11 mmol dm^{-3}. Light scattering measurements indicated that "flowerlike" micelles were formed when two B chains from each conjugate entered the micelle core. Further association of the micelles was found for the conjugates containing more than two BE chains per dendrimer. Drug solubilization in micellar solutions of the conjugates was mainly by the incorporation of drug molecules in micelle cores, with marginal enhancement of solubility attributable to encapsulation in the dendritic micelle coronas. The solubility of hydrophobic drugs in 1 wt % micellar solutions was increased up to 6-fold. Solubilization of ionic drugs was unfavorable due to the limited penetration of ionized drug molecules into the micelle cores.

Introduction

Dendrimers are hyperbranched macromolecules with a well-defined structure and accessible surface groups. Poly(amidoamine) (PAMAM) dendrimers are the first complete dendrimer family to be synthesized and extensively investigated.[1−3] Full generation PAMAM dendrimers are composed of an ethylenediamine (EDA) core, a number of amidoamine branches, and end amino groups. PAMAM dendrimers have attracted considerable interest for their potential applications in pharmaceutical fields such as drug delivery, drug encapsulation, diagnostics, and gene delivery.[3−6]

Their unique dendritic structure and multifunctional surface makes dendrimers ideal drug carriers. Channels and cavities are formed in the interior of the dendrimer molecules and provide a domain for incorporation of hydrophobic guest molecules. Drug molecules can also be attached to the surface of a dendrimer by covalent binding[7,8] or through electrostatic interaction or hydrogen bonding.[9−12]

Poly(ethylene glycol) (PEG) has been used to modify PAMAM dendrimers to enhance their solubilizing ability. The hydrophilic PEG shell also reduces their toxicity and improves their biocompatibility. Kojima and co-workers have reported the modification of PAMAM dendrimers using MPEG chains with different molar masses.[13] The surface of the modified dendrimer molecule was saturated by PEG chains. Solubility studies showed that up to 6.5 adriamycin or 26 methotrexate molecules were incorporated into each dendrimer. The release of methotrexate from the PEGylated dendrimers was related to the ionic strength. Pan and co-workers have examined the loading capacity and release characteristics of PEGylated G3 PAMAM dendrimers using methotrexate as the model drug.[14] It was found that the degree of PEG substitution had little effect on the loading capacity, which indicated that the drug tended to be incorporated within the dendrimer. The degree of substitution showed a negligible effect on the release of loaded drug molecules. The influence of PEG chain length on the drug loading efficiency was investigated by Yang and co-workers.[15] No obvious relationship was found between the loading capacity and PEG chain length. The PEG 2000 dendrimer conjugate exhibited better loading efficiency than the PEG 750 and PEG 5000 conjugates.

Linear−dendritic block copolymers have emerged as an interesting class of dendrimer derivatives for use in drug solubilization. The majority of the linear−dendritic copolymers reported have PEG as the hydrophilic block and a hydrophobic dendritic block, usually a dendron. Gitsov and Fréchet have reported the synthesis of diblock or triblock copolymers composed of a PEG block and a hydrophobic dendritic poly(benzyl ether) block.[16,17] These amphiphilic copolymers form micelles with a dense nanoporous aromatic polyether core and a loose PEG corona.[18] Complexes of the micelles with aromatic compounds showed good stability in aqueous solution. PEG-based block copolymers with dendritic poly(L-lysine),[19] polycarbosilane,[20] and triazine[21] blocks have also been reported. All these copolymers were able to micellize in aqueous solution and could be used for drug encapsulation. Hydrophilic PAMAM-*block*-PEG-*block*-PAMAM triblock copolymers were synthesized by Kim and co-workers and investigated as gene carriers.[22] Their highly water-soluble polyplexes with plasmid DNA had low cytotoxicity despite their poor degradability. A series of dendritic−linear−dendritic triblock copolymers consisting of PAMAM dendron and poly(propylene oxide) has been synthesized by Nguyen and Hammond.[23] Critical micelle concentration (cmc) measurements indicated that these copolymers could self-assemble in aqueous solution at very low concentrations. High loading efficiencies for triclosan were achieved in solubility studies.

In this study we prepared a novel class of linear−dendritic block copolymers by attaching diblock copoly(oxyalkylene) chains to the surfaces of full generation PAMAM dendrimers. Block copoly(oxyalkylene)s, comprising a hydrophilic poly(ethylene oxide) (E) block and a hydrophobic block, for example, poly(propylene oxide) (P), poly(1,2-butylene oxide) (B), or poly(styrene oxide) (S),

*To whom correspondence should be addressed. E-mail: ZZhou2@UClan.ac.uk.

 Published on Web 08/21/2009

Table 1. Molecular Characteristics of the Copolymers[a]

copolymer	M_n/g mol^{-1}	w_B	M_w/M_n	M_w/g mol^{-1}
B_8E_{41}[b]	2380	0.242	1.14	2710
$B_{16}E_{42}$	3070	0.384	1.12	3440

[a] w_B = weight fraction of poly(oxybutylene). M_w is calculated from M_n and M_w/M_n. [b] From ref 32.

are nonionic polymeric surfactants, which can self-associate in dilute aqueous solution.[24] The synthesis and micelle properties of block copoly(oxyalkylene)s have been widely investigated and are well understood.[24−26] The micellar solutions of copoly(oxyalkylene)s possess good thermodynamic stability as indicated by the low values of their cmc. Recent solubilization studies indicated that solubility enhancement for poorly water-soluble drugs can be achieved in micellar solutions of block copoly(oxyalkylene)s of 1 wt % concentration at ambient temperatures.[27−29] In this work, we chose diblock poly(butylene oxide)−poly(ethylene oxide) (BE) copolymers for conjugation with PAMAM dendrimer because oxybutylene units have much higher hydrophobicity than oxypropylene units, and copolymers with relatively short chains micellize well. S units (from styrene oxide) are even more hydrophobic but are less readily synthesized. The sequence of polymerization, butylene oxide followed by ethylene oxide, ensured that the E block had a chemically active hydroxyl end group available for attachment to the dendrimer. It was expected that amphiphilic BE−PAMAM dendrimer conjugates would self-associate to form micelles in aqueous solution with poly(butylene oxide)s in the core and PAMAM dendrimers in the periphery. The combination of block copolymer micelles and the dendritic architecture of PAMAM dendrimer could provide multiple sites for drug encapsulation: the hydrophobic core, the ethylene oxide branches, and the dendritic corona.

The specific objectives of this study were to synthesize and characterize a series of BE−PAMAM dendrimer conjugates, to use light scattering techniques to investigate the micellization behavior of the conjugates in aqueous solution, and to determine the solubilization capacities of the conjugates for poorly water-soluble drugs under appropriate conditions by a convenient UV assay.

Experimental Section

BE Block Copolymers. The copolymers were prepared by sequential oxyanionic copolymerization of butylene oxide followed by ethylene oxide. The preparation of copolymer B_8E_{41} has been described in detail previously.[30] Copolymer $B_{16}E_{42}$ was prepared using a similar method. The initiator was 2-butanol partly converted to its potassium salt (ratio [OH]/[K$^+$] ≈ 9). Freshly distilled butylene oxide was transferred under vacuum into the ampule and heated at successively, 45 °C (5 days) and 65 °C (21 days). Then ethylene oxide was distilled into the ampule and held at 65 °C for about 3 weeks until conversion was complete. The copolymer was characterized by gel permeation chromatography (GPC, tetrahydrofuran eluent, detected by differential refractometer, calibrated with poly(oxyethylene) standards) for determination of the ratio of weight-average to number-average molar mass (polydispersity, M_w/M_n) and by ^{13}C NMR spectroscopy (Varian Unity 500 spectrometer) for determination of the absolute value of M_n and confirmation of the diblock architecture. Details of the methods have been published.[31,32] Values of the molecular characteristics are listed in Table 1. The polydispersity is narrow and is acceptable for the purpose of this study.

BE−PAMAM Dendrimer Conjugates. *Materials.* Generation 1−3 PAMAM dendrimers with ethylenediamine cores (20% w/v in methanol) were purchased from Dendritech Inc. (Midland, MI). 4-Nitrophenyl chloroformate (NPC) (97%), tetrahydrofuran (THF), and dimethyl sulfoxide (DMSO) were purchased from Sigma-Aldrich (UK). Triethylamine (TEA) (99%) was obtained from Lancaster Synthesis (UK). Hexane, diethyl ether, and chloroform were GPR grade and used directly without further purification. Whatman No. 1 filters were from Whatman (Kent, UK). Samples of Visking tubing with molecular weight cutoff (MWCO) 3500, 7000, and 12 000−14 000 g mol^{-1} were obtained from Medicell International, UK.

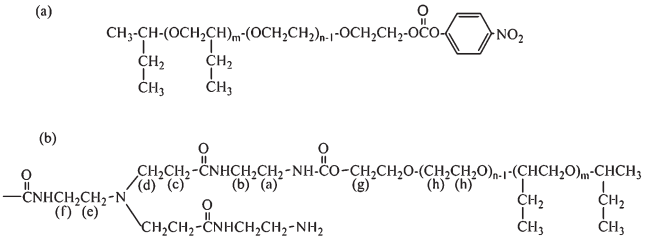

Figure 1. Structures of (a) BE−NPC carbonate and (b) BE−dendrimer conjugate.

Scheme 1. Synthesis of BE−Dendrimer Conjugates: (a) Activation of BE Copolymer and (b) Conjugation with PAMAM Dendrimer

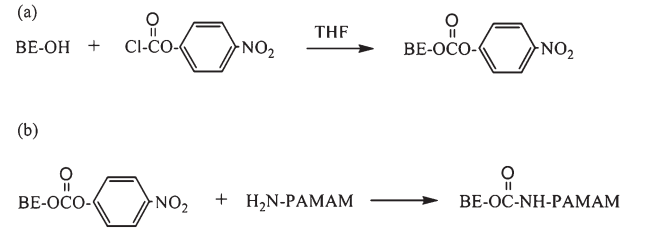

BE−PAMAM dendrimer conjugates were characterized by ^{1}H and ^{13}C NMR spectroscopy (Bruker Avance 300, Bruker, Coventry, U.K.). NMR grade chloroform-*d* and methanol-*d* were from Cambridge Isotope Laboratories. The assignment for the peaks of PAMAM dendrimer in the ^{1}H and ^{13}C spectra was made according to relevant references[13,33] and with the aid of 2D COSY NMR.

Synthesis of BE−4-Nitrophenyl Carbonate. The hydroxyl groups on the E ends of BE copolymers were activated by reaction with 4-nitrophenyl chloroformate (Scheme 1a). Briefly, BE copolymer (0.75 mmol) was completely dissolved in 40 mL of anhydrous THF at room temperature. 4-Nitrophenyl chloroformate (1.5 mmol) was added portion-wise to the solution. Triethylamine (1.5 mmol) was added, and the mixture was stirred at room temperature for 3 days. The salt in the reaction mixture was filtered off, and the filtrate was evaporated under reduced pressure. The crude product was purified by repeated precipitation in diethyl ether−hexane (1:10) and dried under vacuum. Yield: 77−84%. ^{1}H NMR ($CDCl_3$): 0.80−1.00 (m, CH_3−), 1.28−1.71 (m, CH_3CH_2−), 3.22−3.91 (m, backbone −CHO− and −CH_2O−), 4.40 (t, −CH_2OCOO−), 7.38 (d, Ar), 8.36 (d, Ar). ^{13}C NMR ($CDCl_3$): 9.6 (CH_3CH_2−), 19.0 (CH_3CHO−), 24.6 (CH_3CH_2−), 29.0 ($CH_3CH(CH_2CH_3)$O−), 68.2 (−CH_2OCOO−), 69.0−82.0 (backbone −CHO− and −CH_2O−), 121.5, 125.7, 145.6, 152.8 (Ar), 155.1 (−OCOO−).

Synthesis of BE−Dendrimer Conjugates. The structure of BE−dendrimer conjugate is shown in Figure 1. The activated copolymers were attached to the surface amino groups of PAMAM dendrimer (Scheme 1b). Briefly, PAMAM dendrimer (0.4 mmol) was dried under vacuum and dissolved in 40 mL of anhydrous dimethyl sulfoxide (DMSO) at room temperature. An appropriate amount of BE 4-nitrophenyl carbonate (BE-NPC) previously dissolved in 10 mL DMSO was added portion-wise to the solution. The mixture was stirred at room temperature for 5 days. The solution was then diluted and dialyzed against distilled water for 5 days using a dialysis tubing. The dilution was filtered and lyophilized. The residue was dissolved in distilled water and purified by extracting three times with chloroform.

The solution was then dried under vacuum. Yield: 41−53%. ^{1}H NMR (MeOD): 0.80−1.00 (m, CH_3−), 1.28−1.71 (m, CH_3CH_2−), 2.31−2.45 (m, $-CH_2CONH-(c)$), 2.49−2.66 (m, $=NCH_2CH_2N=$, $-NHCH_2CH_2N=(e)$), 2.69−2.92 (m, $-NHCH_2CH_2NH_2$, $=NCH_2CH_2CO-(d)$), 3.18−3.90 (m, $-CH_2NHCOO-(a)$, $-CONHCH_2CH_2NH_2$, $-CONHCH_2CH_2NH-(b)$, $-CONHCH_2CH_2N=(f)$, BE backbone −CHO− and $-CH_2O-(h)$), 4.15 (t, $-NHCOOCH_2-(g)$). ^{13}C NMR (MeOD): 10.3, 19.5, 25.8, 30.4 (side and head CH_3−, CH_3CH_2− of B block), 34.8 ($-CH_2CONH-(c)$), 39.0 ($-CONHCH_2CH_2N=(f)$), 42.1 ($-CONHCH_2CH_2NH-(b)$), 42.6 ($-CH_2NHCOO-(a)$), 51.6 ($=NCH_2CH_2CO-(d)$), 54.1 ($-NHCH_2CH_2N=(e)$), 65.5 ($-NHCOOCH_2-(g)$), 70.0−83.0 (backbone −CHO−, $-CH_2O-(h)$), 158.9 (−NHCOO−), 174.9, 175.3 (−CONH−).

Critical Micelle Concentration (cmc). The cmcs of the BE−PAMAM dendrimer conjugates in aqueous solution were measured at 25 °C using pyrene as the probe. Solutions were prepared in aqueous phosphate buffer (0.067 M, pH 7.4) to control the ionization of the dendrimer. Excess pyrene (20 mg, Sigma-Aldrich) was added to 2 mL samples of micellar solutions ranging in concentration from 0.005 to 1 wt %. The solutions were kept at 25 °C for 3 days and then filtered. The absorbance of the filtrate was measured at 272 nm using a UV−vis spectrometer (Cecil CE1021), and the cmcs of the BE−dendrimer conjugates were determined from the dependence of absorbance on concentration.

Light Scattering. Static and dynamic light-scattering techniques were used to determine micelle properties of the BE copolymers and their dendrimer conjugates. The micellar solutions of copolymer $B_{16}E_{42}$ in the concentration range 5−60 g dm^{-3} were prepared in distilled water, and the solutions of the BE−PAMAM dendrimer conjugates with the concentration 2.5−30 g dm^{-3} were prepared in aqueous phosphate buffer (0.067 M, pH7.4). The solutions were optically clear under the conditions of measurement.

In an experiment, solutions were clarified by filtering through Millipore Millex filters (0.22 μm porosity) directly into scattering cells previously cleaned with condensing acetone vapor. Static light scattering (SLS) intensities were measured at temperatures in the range of 15−35 °C by means of a Brookhaven BI200S instrument using vertically polarized incident light of wavelength 488 nm supplied by an argon ion laser (Coherent Innova 90) operated at 500 mW or less. The intensity scale was calibrated against scattering from benzene, and the scattering angle was 90° to the incident beam. Analysis of the SLS data was based on the Debye equation,

$$K^*c/(I-I_s) = 1/M_w + 2A_2c... \quad (1)$$

where I is intensity of light scattering from solution relative to that from benzene, I_s is the corresponding quantity for the solvent, c is the concentration (in g dm^{-3}), M_w is the weight-average molar mass of the solute, A_2 is the second virial coefficient (higher coefficients being neglected), and K^* is the appropriate optical constant, which includes the specific refractive index increment, dn/dc. Values of dn/dc were determined by means of an Abbé 60/ED precision refractometer (Bellingham and Stanley Ltd., UK.). Debye plots were used to obtain values of the weight-average molar mass of the micelles ($M_{w,mic}$) by extrapolation to zero concentration and of the corresponding thermodynamic radius (effective hard sphere) of the micelles.

Dynamic light scattering (DLS) measurements were made with the same instrument, using a Brookhaven BI9000AT digital correlator to acquire data. The correlation functions from DLS were analyzed using the CONTIN program[34] to obtain intensity fraction distributions of the apparent diffusion coefficient (D_{app}) and hence of the apparent hydrodynamic radius ($r_{h,app}$, radius of the hydrodynamically equivalent hard sphere) via the Stokes−Einstein equation,

$$r_{h,app} = kT/(6\pi\eta D_{app}) \quad (2)$$

where k is the Boltzmann constant and η is the viscosity of water at temperature T. Extrapolation of the values of $1/r_{h,app}$ to zero concentration gave true values of the hydrodynamic radius (r_h).

Drug Solubilization. The solubilization capacities for two model drugs (carbamazepine and spironolactone, Sigma-Aldrich Co.) in micellar solutions of the BE dendrimer conjugates at 25 °C were investigated. For comparison, the solubilities of the model drugs in micellar solutions of B_8E_{41} and $B_{16}E_{42}$ and in solutions of unmodified G1−3 PAMAM dendrimers were measured under the same conditions. Stock 1 wt % micellar solutions of the copolymers and conjugates were prepared in phosphate buffer (pH 7.4, 0.067 M). The pH values of the solutions were measured by a pH meter (Fisher Scientific Accumet basic), and if needed, a few drops of HCl were added to adjust the pH value to 7.4.

Saturated drug-loaded solutions were prepared in glass vessels by mixing excess powdered drug (10 mg) with 2 mL of 1 wt % micellar solution. The vessels were placed into a water bath (Grant Instruments) at 25 °C and stirred for 3 days before being filtered (0.45 μm Millipore) to remove any unsolubilized drug. Blank experiments (no polymer) gave the solubility of drug in buffer solution. The amount of drug solubilized was determined by UV assay. The filtrate was diluted 50 times with a mixed solvent (acetonitrile/water/trifluoroacetic acid, 50/50/0.1), and the UV absorbance was determined at optimum wavelength: 242 nm for spironolactone and 285 nm for carbamazepine. Calibration with drug alone gave satisfactory Beer′s law plots. All measurements were carried out in triplicate and the results averaged. The stability of drugs during solubilization was monitored by HPLC in a separate study: the evidence was that spironolactone and carbamazepine were free from breakdown products after 3 days equilibration.[29]

Results and Discussion

Synthesis and Characterization of BE Dendrimer Conjugates. As shown in Scheme 1, the hydroxyl group of BE copolymer was activated by NPC via a carbonate bond. Excess NPC and unreacted BE copolymers were sufficiently removed by solvent extraction. Any residual BE copolymers are not able to react with PAMAM dendrimer in the following reaction and cannot disturb the conjugation. PAMAM dendrimer is conjugated to BE copolymer via a nucleophilic attack on the carbonyl group, and a carbamate bond is formed. Most small molecules and unreacted polymers were removed by dialysis against distilled water. However, the process was slow as unreacted polymers could micellize in aqueous solution and did not easily pass through the dialysis membrane, although polymer and dendrimer molecule were small enough to penetrate. However, residual 4-nitrophenol and free BE polymers could be completely removed by repetitive extraction with chloroform.

In the ^{1}H and ^{13}C NMR spectra, change in chemical shift before and after conjugation of the end methylene group of the BE copolymer (next to the hydroxyl end group) confirmed the formation of BE−NPC carbonate and of BE−dendrimer conjugate. Although different NMR solvents were used for characterization, comparison could be made directly between the spectra of BE copolymer, BE−NPC, and BE−PAMAM conjugates.

In the ^{1}H NMR spectrum of BE copolymer (Figure 2a), the peak of the end CH_2 group overlaps with the peaks of CH_2 in the E backbone. However, in the ^{13}C NMR spectrum, the peak of the end CH_2 is at 61.4 ppm and well separated from the other peaks.[31] After coupling with NPC, the hydroxyl group was replaced by a carbonate link. A new peak appeared in the ^{1}H spectrum (Figure 2b) at 4.40 ppm, which corresponds to the end CH_2 group, while the peaks between 7.4 and 8.3 ppm are from the protons of phenyl

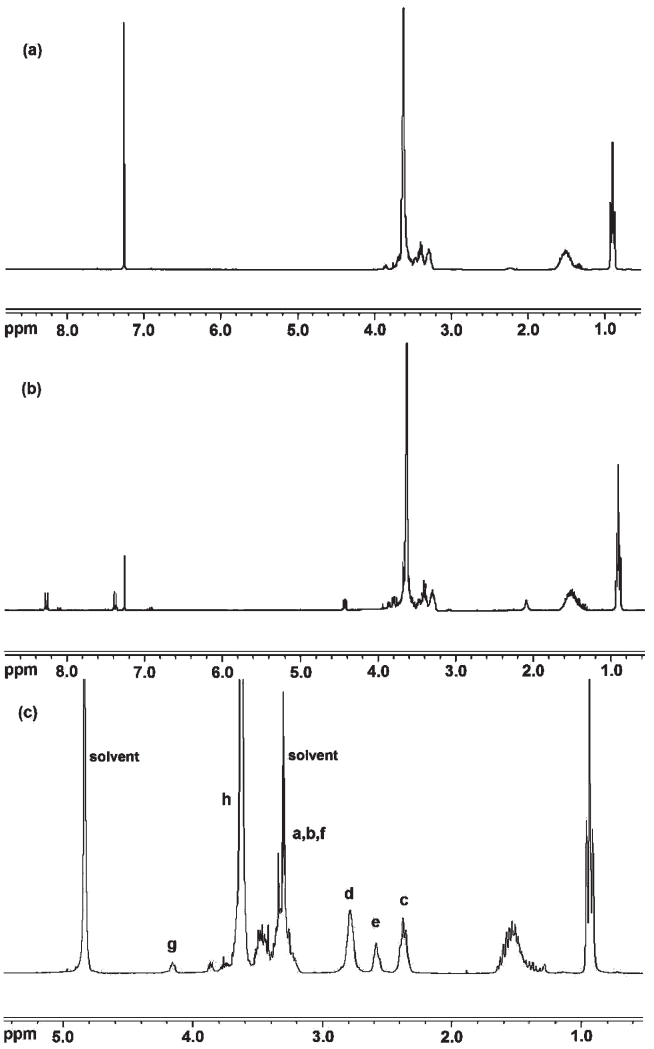

Figure 2. ^{1}H NMR spectra of (a) BE copolymer, (b) BE−NPC carbonate, and (c) BE−dendrimer conjugate.

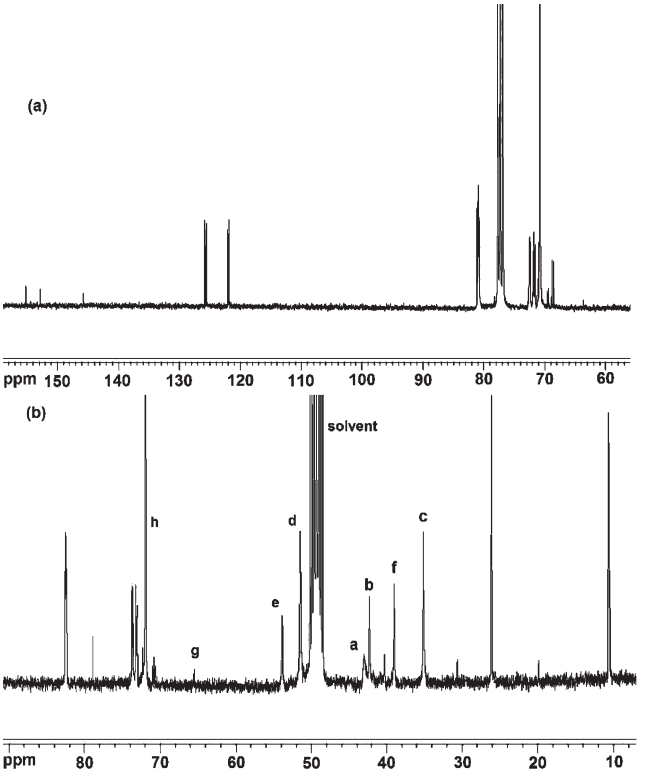

Figure 3. ^{13}C NMR spectra of (a) BE−NPC carbonate and (b) BE−dendrimer conjugate.

Table 2. Molecular Characteristics of BE−PAMAM Dendrimer Conjugates[a]

	molar ratio of BE/dendrimer	M_n (g mol^{-1})	B (wt %)
$B_{16}E_{42}$−G2	2.0	9400	24.5
$B_{16}E_{42}$−G3a	1.5	11 500	15.0
$B_{16}E_{42}$−G3b	3.0	16 100	21.4
B_8E_{41}−G1	2.1	6500	18.7
B_8E_{41}−G2	1.8	7600	13.7

[a] Estimated uncertainties: MW, ±5%; wt % B, ±1%.

group. In the ^{13}C spectrum (Figure 3a), a shift of the peak of the end CH_2 group from 61.4 to 68.2 ppm indicates the formation of BE−NPC carbonate. When conjugating with PAMAM dendrimer, a carbamate bond was formed. The peak of the end CH_2 group shifted from 4.40 to 4.15 ppm in the ^{1}H spectrum (Figure 2c) and from 68.2 to 65.5 ppm in the ^{13}C NMR spectrum (Figure 3b). The absence of peaks above 7 ppm in the ^{1}H spectrum of the BE−dendrimer conjugates suggests that the aromatic byproduct were completely removed from the conjugates, while the absence of peaks at 61.4 and 68.2 ppm in the ^{13}C NMR spectrum indicated that no free BE copolymers remained. In the ^{13}C NMR spectrum, the activation of BE copolymer by NPC was confirmed by the appearance of a new carbonyl peak at 155.1 ppm. Similarly, the formation of BE−dendrimer conjugates was confirmed by a carbamate carbonyl peak at 158.9 ppm.

Five conjugates of BE copolymers with PAMAM dendrimers of different generations were prepared. Low generation dendrimers (G1−G3) were preferred to reduce steric hindrance in the periphery of micelles. The molar ratios of B block to dendrimer were carefully chosen to ensure the formation of micelles while achieving appropriate hydrophilicity. The average number of BE chains per PAMAM dendrimer molecule was determined from the ^{1}H NMR spectrum (Figure 2c) by comparing the integrals of the CH_2 end group of BE copolymer (peak *g*) and the CH_2 group next to the carbonyl group of PAMAM dendrimer (peak *c*), and then the number-average molar mass and B-content were calculated. The molecular characteristics of the BE−dendrimer conjugates are listed in Table 2.

Critical Micelle Concentration. The aggregation behavior of the BE copolymers and the BE−PAMAM dendrimer conjugates in aqueous solution was investigated in this study. Previous research shows that copolymer B_8E_{41} can self-associate in very dilute aqueous solution (0.1 g dm^{-3}) and is completely micellized in 1 wt % aqueous solution at room temperature.[32] The correlation of critical micelle concentrations with B-block length[25] indicates that the cmc of copolymer $B_{16}E_{42}$, with long hydrophobic block length, is sufficiently low under the conditions of the study.

The critical micelle concentrations of the BE dendrimer conjugates were measured in aqueous phosphate buffer solution (0.067 M, pH7.4) in order to control the ionization of dendrimer. Those of the BE copolymers were measured in the same buffer: compared with water the effect of buffer was negligible because the ionic strength was low.

The plot of absorbance versus logarithm concentration for copolymer B_8E_{41} shown in Figure 4, is typical for the BE block copolymers and the BE−PAMAM conjugates prepared in this work. When the concentration increases above a certain value, the absorbance rises from the baseline and increases more rapidly as concentration is increased.

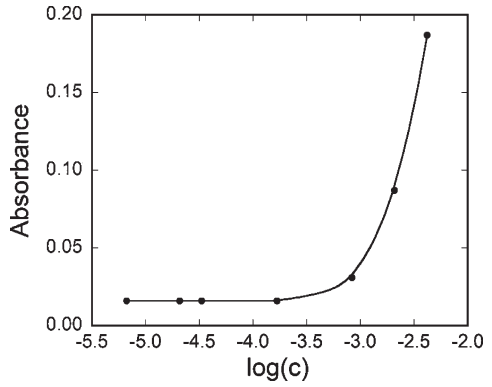

Figure 4. Absorbance vs logarithm concentration (mol dm^{-3}) for diblock copolymer B_8E_{41} at 25 °C.

Table 3. Cmc Data for the BE Copolymers and BE−PAMAM Conjugates at 25 °C[a]

	cmc	
	(mmol dm^{-3})	(g dm^{-3})
B_8E_{41}	0.44	1.06
$B_{16}E_{42}$	0.10	0.31
B_8E_{41}−G1	0.11	0.79
B_8E_{41}−G2	0.089	0.67
$B_{16}E_{42}$−G2	0.040	0.37
$B_{16}E_{42}$−G3a	0.020	0.23
$B_{16}E_{42}$−G3b	0.018	0.29

[a] Estimated error cmc ±10%.

The commencement of curvature is used as an indication of the start of the micellization process. The cmc values of the BE copolymers and BE−PAMAM conjugates are listed in Table 3. The cmc of B_8E_{41} measured by surface tension was reported to be 1.0 g dm^{-3} at 26 °C.[32] Comparing with the value measured by solubilization (1.06 g dm^{-3} at 25 °C), it is concluded that the results from these two methods are in good agreement.

It is shown in Table 3 that the cmcs of the BE−PAMAM dendrimer conjugates are lower than those of their component BE copolymers when considered in molar units due to the conjugation of more than one polymer chain per dendrimer molecule. The dendrimer molecule is hydrophilic especially with the surface amino groups ionized, which partially compensates the conjugates for the loss of hydrophilicity. Similar to BE copolymers, the cmcs of the BE−PAMAM conjugates are mainly determined by their core-forming hydrophobic B blocks. The plot of cmc against molar ratio of BE to dendrimer (Figure 5) indicates that the cmcs of the BE−PAMAM conjugates are dependent on the B-block length and are irrespective of the molar ratio and the size of dendrimer.

Micelle Properties. Dynamic light scattering from buffered solutions of the two B_8E_{41}−dendrimer conjugates at different concentrations and temperatures was analyzed by the CONTIN program to obtain intensity fraction distributions of $\log(r_{h,app})$. Distribution curves for a 10 g dm^{-3} buffer solution of the B_8E_{41}−G2 conjugate at several temperatures are illustrated in Figure 6. The distributions are narrow and single-peaked, which is taken as evidence of closed association of the B_8E_{41}−G2 conjugate to form spherical micelles in solution. It is also found that the width of the peak becomes narrower with increasing temperature. Considering that the cmc of the B_8E_{41}−G2 conjugate is low (0.67 g dm^{-3} at 25 °C), most molecules should exist in the form of micelles in solution at 25 °C or higher. The narrow distributions and the shift to higher values of $r_{h,app}$ found for the solution of the

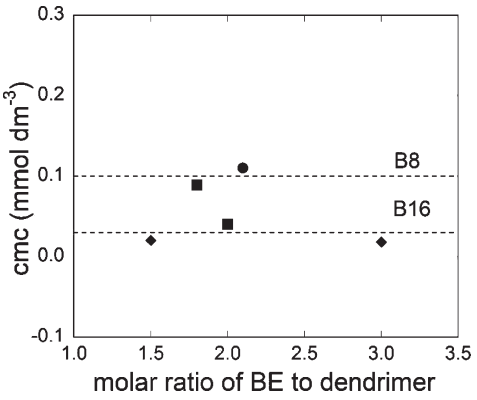

Figure 5. Dependence of cmc on molar ratio of BE to dendrimer for BE−PAMAM conjugates: (●) G1 conjugate, (■) G2 conjugates, and (◆) G3 conjugates.

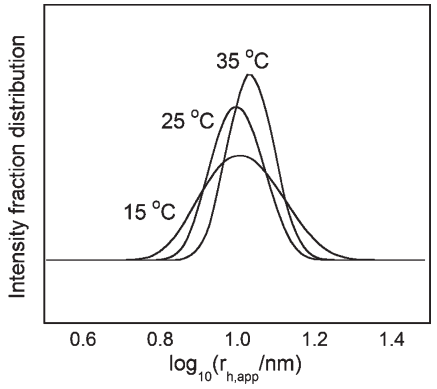

Figure 6. Intensity fraction distributions of logarithm apparent hydrodynamic radius of micelles in a 10 g dm^{-3} buffer solution of the B_8E_{41}−G2 conjugate in buffer at the temperatures indicated.

B_8E_{41}−G2 conjugate between 25 and 35 °C are consistent with full micellization of the molecules and the growth of micelles with temperature. The B_8E_{41}−G1 conjugate in buffer solution behaves similarly to B_8E_{41}−G2. Single peaks centered on $\log(r_{h,app}) \approx 1$ indicate the formation of spherical micelles. The values of r_h at 25 °C obtained by plotting the reciprocal of the intensity-average apparent hydrodynamic radius against concentration are listed in Table 4.

The DLS study of the three $B_{16}E_{42}$−dendrimer conjugates showed a more complicated micellization behavior. A comparison of the intensity fraction distributions of $\log(r_{h,app})$ for 10 g dm^{-3} buffer solutions of the five BE−dendrimer conjugates at 25 °C is illustrated in Figure 7. The micelle size distribution curves of $B_{16}E_{42}$−G2 and $B_{16}E_{42}$−G3a show two well-defined peaks. The peak at ca. 12 nm is assigned to spherical micelles while the large peak (> 30 nm) is probably related to aggregates of spherical micelles. However, for the conjugate $B_{16}E_{42}$−G3b, which has an average of three BE chains per molecule, the plot of size distribution shows that a continuous distribution of structures is formed and a very broad peak is found between 8 and 40 nm, possibly because there are steric constraints to forming even simple micellar structures, which tends to cause formation of micelle network and broadens the distribution. Although the intensity fraction for the micelle aggregates is very high, the proportion of molecules forming spherical micelles is dominant because the intensity is dependent on the weight fraction and the molar mass of micelles. As the molar mass of micelle aggregate is higher than that of spherical micelle, the weight fraction and hence the number proportion of micelle aggregate are small.

Table 4. Micelle Properties of BE−PAMAM Dendrimer Conjugates and BE Copolymers in Aqueous Buffer Solution[a]

	T/°C	$M_{w,mic}/10^5$ g mol^{-1}	N_w	r_t/nm	r_h/nm	dn/dc/mL/g
B_8E_{41}−G1	15	2.3	36	6.5		0.147
	25	2.65	41	7.0	8.7	0.144
	35	3.2	49	7.5		0.139
B_8E_{41}−G2	15	1.32	17	5.9		0.165
	25	2.5	33	8.0	10.0	0.161
	35	2.95	39	8.6		0.158
$B_{16}E_{42}$−G2	25	8.2	87			0.156
	35	8.5	90			0.152
$B_{16}E_{42}$−G3a	25	8.6	75			0.167
	35	8.8	76			0.164
$B_{16}E_{42}$−G3b	25	6.4	40	10.5	16.7	0.159
	35	6.5	40	10.5		0.156
B_8E_{41}[b]	25	1.4	52	5.7	9.3	
	35	1.8	66	6.3	9.0	
$B_{16}E_{42}$	15	5.05	164	9.1	10.9	0.136
	25	5.45	177	9.2	10.8	0.134
	35	5.7	185	9.3	10.8	0.132

[a] Estimated uncertainties: ±1 in r_h and r_t ; ±10% in $M_{w,mic}$ and N_w. [b] Values from ref 32.

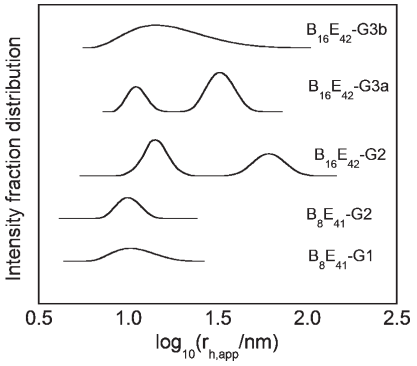

Figure 7. Comparison of micelle size distributions of a 10 g dm^{-3} solution of BE−PAMAM dendrimer conjugates (as indicated) in buffer at 25 °C.

Debye plots were used to determine the average molar masses, association numbers, and thermodynamic radii of the micelles of the BE copolymers and BE−PAMAM dendrimer conjugates. Examples of Debye plots are shown in Figure 8. The curves were fitted based on scattering theory for hard spheres using the Carnahan−Starling analysis.[35] Values obtained for the weight-average molar mass of the micelles, the weight-average association number of the micelles, N_w defined as $M_{w,mic}/M_w$, where M_w is the weight-average molar mass of the unassociated copolymer or conjugate molecules (unimers), and the corresponding average micelle radii are listed in Table 4. Copolymer B_8E_{41} was reported to form spherical micelles in aqueous solution.[30] The micelle properties of $B_{16}E_{42}$ are similar to those of B_8E_{41}, although the relatively large value of N_w indicates that the micelle size has almost reached the limit for spherical micelles. The values of r_t, which essentially reflect the excluded volume of the fringe of the micelle, are more or less independent of temperature. This could be explained as a compensation between an increase in micelle molar mass and a decrease in thermodynamic expansion factor.

As seen in Table 4, the association numbers and the thermodynamic radii of the B_8E_{41}−dendrimer conjugates increase consistently with increasing temperature, which corresponds to the growth of spherical micelles at higher temperatures as illustrated in Figure 6. However, the micelle properties of the $B_{16}E_{42}$−dendrimer conjugates show less dependence on temperature, which is consistent with values

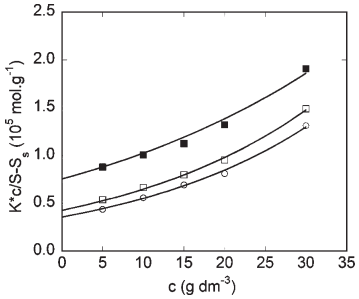

Figure 8. Debye plots for aqueous buffer solutions of the B_8E_{41}−G2 conjugate at (■) 15, (□) 25, and (○) 35 °C.

of N_w being near the limit for the core radius of spherical micelles when the B-block length is B_{16}. Figure 7 illustrates that micellar solutions of the $B_{16}E_{42}$−dendrimer conjugates contain a mixture of different species of micelles and the hard-sphere model may not be strictly applicable for these conjugates although an average value of the radius still can be estimated if all the particles are treated as spherical.

Micelle Structure and Shape. As determined by ^{1}H NMR, most of the BE−PAMAM dendrimer conjugates have approximately two BE polymer chains attached to dendrimer. A BE−dendrimer conjugate with two BE chains per molecule is actually a BE−dendrimer−EB triblock copolymer, i.e., a copolymer with a hydrophilic inner block and hydrophobic end blocks, similar to a $B_nE_mB_n$ triblock copolymer. The association properties of BEB copolymers are well understood.[36−38] At high dilution the BEB chains loop to form micelles with a B-block core and an E-block corona: so-called "flowerlike" micelles. At higher concentrations a proportion of copolymer chains extend to form bridges between two micelles and at yet higher concentrations to form small bridged networks. These are equilibrium structures, i.e., the bridges are dynamic in nature, and the bridged structures contribute a broad second peak to the distribution of particle radii.

With similar block architecture, the BE−dendrimer conjugate is considered to show the same micellization behavior as $B_nE_mB_n$ triblock copolymer. Considering that the sizes of low-generation dendrimers are much smaller than the chain length of BE copolymer, then during micellization the two polymer chains in the molecule of the conjugates tend to fold back to form a loop with the two B ends attached together. Consequently, the spherical micelle formed is a cluster of loops with hydrophobic B blocks as the micelle core and dendrimers as the periphery. The structure of spherical micelle is illustrated schematically in Figure 9, which is an idealized model since the chain length distribution in the B block is not negligible.

The structure of micelle is confirmed to be reasonable by the following calculations. Table 4 shows that the association number of B_8E_{41}−G2 at 35 °C is 39, which means there are ca. 80 B_8 blocks in a micelle core. The specific volume of poly(oxybutylene) at 35 °C is 1.040 cm^3 g^{-1},[39] and so the average core volume of micelles with B_8 core blocks is ~80 nm^3 and, if spherical, the micelles would have a radius of 2.7 nm. Given 0.363 nm per B unit,[40] the length of a B_8 block is only 2.9 nm, and so it is within the limit of a spherical core size. Also, the thermodynamic radius of B_8E_{41}−G2 at 35 °C is 8.6 nm, and so the thermodynamic surface area and volume of a micelle, if spherical, are 930 nm^2 and 2660 nm^3, respectively. The diameter of G2 PAMAM dendrimer is 3 nm, and thus the 40 G2 dendrimers on the surface of a micelle only occupy 280 nm^2 surface area and 420 nm^3 volume. Hence, the dendrimer molecules are well scattered

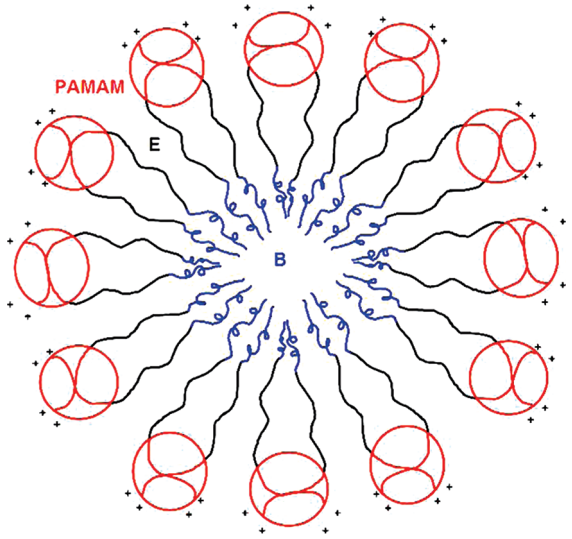

Figure 9. Schematic illustration of structure of spherical micelle formed by BE−PAMAM conjugates.

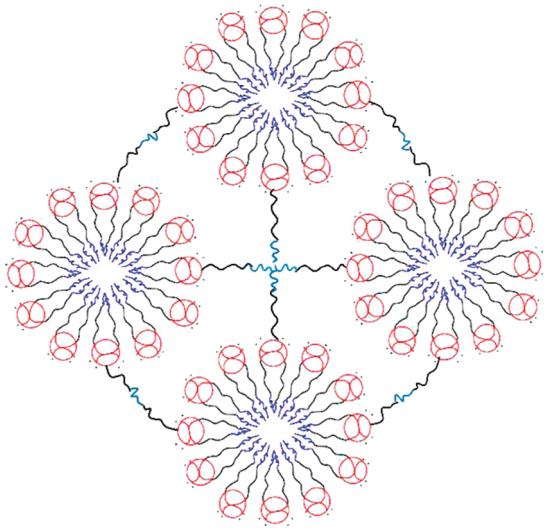

Figure 10. Schematic illustration of structure of micelle aggregate formed by BE−PAMAM dendrimer conjugates.

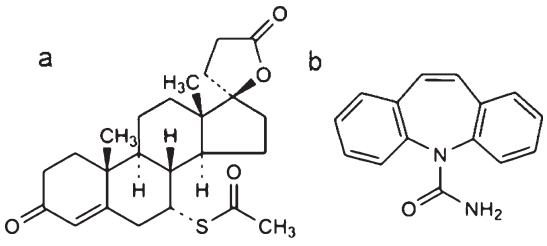

Figure 11. Molecular structure of spironolactone (a) and carbamazepine (b).

on the surface of the micelles, and there is no significant steric or electrostatic repulsion between the dendrimers on the micelle surface.

The distributions from DLS indicate that large micelles exist in solutions of $B_{16}E_{42}$−dendrimer conjugates in addition to spherical micelles. The number of BE chains per dendrimer is an average value, which means that there is still a small proportion of molecules with more than two chains in the sample although those with two polymer chains are dominant. It is not possible for all the chains to fold back into the micelle core, especially for the conjugates with large generation dendrimer, which will maximize the entropy. Furthermore, it is also considered to be very difficult for every BE chain in a conjugate molecule to enter the core of a different micelle. This is because dendrimer molecules in the fringe have a relatively rigid structure and bear positive charges, and thus appreciable steric hindrance and electrostatic repulsion will be produced if the micelles get too close. Hence, the additional BE chains will associate with each other and lead to a further aggregation of spherical micelles (Figure 10). The aggregation of micelles is more likely to occur for the conjugates having longer BE chains (due to the wide distribution of chain length) and smaller dendrimers in order to minimize steric repulsion. If the conjugate molecules are synthesized with more than two polymer chains, e.g., $B_{16}E_{42}$−G3b, there is a tendency for the formation of a network by cross-linking not only between the conjugate molecules but also between the micelles. This explains why a much broader distribution is found for $B_{16}E_{42}$−G3b.

Drug Solubilization. The solubilization of drugs in micellar solutions of the BE−PAMAM dendrimer conjugates was investigated using spironolactone and carbamazepine (pK_a 7.0) as model drugs (Figure 11). Phosphate buffer (0.067 M, pH 7.4) was used to maintain the solutions at a constant (physiological) pH. With a pK_a of ca. 10, the amino groups of PAMAM dendrimers were completely protonated in micellar solution at pH 7.4, and the corona surface of micelles of the dendrimer conjugates was positively charged. The pH values of the saturated drug-loaded solutions were monitored, and the results showed that the buffer provided good pH control.

The solubilization capacity (S_{bp}) was determined as milligram drug per gram of conjugate (mg g^{-1}). The solubility of the drug in the solvent blank (S_0) was subtracted from the solubility (S) in micellar solutions to obtain the amount of drug solubilized in the micelles, S_{bp}. The quantity was calculated from $S - S_0$ in mg dL^{-1}, equivalent to mg g^{-1} for a 1 wt % solution. The solubilization capacities for spironolactone and carbamazepine in 1 wt % micellar solutions at 25 °C are reported in Table 5. The enhancement of solubility (S/S_0) to the solvent blank is also shown in the table.

From the water solubility (S_0), spironolactone is more hydrophobic than carbamazepine and thus more compatible with the hydrophobic core-forming B-block. Carbamazepine has a moderate solubility in buffer solution and is ~28% ionized at pH 7.4. Compared to the enhancement of solubility for spironolactone where $S/S_0 = 4-7$, the solubility of carbamazepine in solutions of the BE−dendrimer conjugates is only doubled, and the penetration of this drug into the micelle core is poor due to its polarity and ionization. The ionized drug molecules are electrostatically repelled by the positively charged surface-primary or interior-tertiary amino groups of the dendrimer. Hence, it is also unfavorable for this drug to be encapsulated in the micelle fringe of the BE−dendrimer conjugates.

As seen in Table 5, the G1−3 PAMAM dendrimers are very poor solubilizers for hydrophobic drugs. The low-generation PAMAM dendrimers have a relatively open structure which water molecules can easily penetrate. The hydrophilic environment is not favorable for incorporation of hydrophobic drugs. The observation of much better solubilization of spironolactone in solutions of copolymers B_8E_{41} and $B_{16}E_{42}$ confirms that the hydrophobic core is the domain for drug solubilization. Copolymer $B_{16}E_{42}$ has a higher hydrophobic content than B_8E_{41} and thus shows

Table 5. Solubilization of Drugs in 1 wt % Micellar Solutions in Phosphate Buffer at 25 °C of BE Copolymers, PAMAM Dendrimers, and BE−PAMAM Dendrimer Conjugates

drug	polymer	S/mg dL^{-1}	S/S_0	S_{bp}[a]/mg g^{-1}
spironolactone	B_8E_{41}	6.51	3.83	4.8
S_0 = 1.7 mg dL^{-1}	$B_{16}E_{42}$	9.71	5.71	8.0
M_w = 416.6 g mol^{-1}	G1 den	2.63	1.55	0.9
	G2 den	2.86	1.68	1.2
	G3 den	2.63	1.55	0.9
	B_8E_{41}−G1	8.68	5.11	7.0
	B_8E_{41}−G2	7.20	4.20	5.5
	$B_{16}E_{42}$−G2	11.88	6.99	10.2
	$B_{16}E_{42}$−G3a	9.37	5.51	7.7
	$B_{16}E_{42}$−G3b	10.17	5.98	8.5
carbamazepine	B_8E_{41}	18.9	1.60	7.1
S_0 = 11.8 mg dL^{-1}	$B_{16}E_{42}$	21.8	1.85	10.0
M_w = 236.3 g mol^{-1}	G1 den	15.0	1.27	3.2
	G2 den	15.4	1.31	3.6
	G3 den	15.2	1.29	3.4
	B_8E_{41}−G1	21.1	1.79	9.3
	B_8E_{41}−G2	19.5	1.65	7.7
	$B_{16}E_{42}$−G2	23.5	1.99	11.7
	$B_{16}E_{42}$−G3a	21.0	1.78	9.2
	$B_{16}E_{42}$−G3b	22.5	1.91	10.7

[a] Estimated uncertainty ±1 mg g^{-1}.

higher solubilization efficiency. A similar tendency is also demonstrated for the BE−dendrimer conjugates.

When compared to values for their component BE copolymers, the solubilization capacities recorded for the BE−dendrimer conjugates show only a marginal increase, e.g., values of S_{bp} for B_8E_{41}−G1 and B_8E_{41}−G2 and spironolactone are only 45% and 15% higher than S_{bp} for copolymer B_8E_{41}. The solubilization capacity expressed as mg g^{-1} is related to the hydrophobic content in the BE−dendrimer conjugates. As the hydrophobic contents of BE copolymers is reduced after conjugating with dendrimers, direct comparison of these results is not entirely appropriate. The solubilization capacities of B_8E_{41}, B_8E_{41}−G1, and B_8E_{41}−G2, in an alternative representation as mole drug molecules per mole of conjugate micelles, are 1.6, 4.5, and 3.3 mol mol^{-1}, respectively, which indicate the number of drug molecules per micelle. The micelles of B_8E_{41}−dendrimer conjugates are able to encapsulate two or three times the number of drug molecules than B_8E_{41}. Considering that the micelles of B_8E_{41} and its dendrimer conjugates have a hydrophobic core of similar size, it is concluded that the enhancement of solubilization partly originates from the micelle corona which can entrap drug molecules in the cavities between the poly(ethylene oxide) or dendrimer branches.

For the $B_{16}E_{42}$−dendrimer conjugates, the solubilization results are subjected to the net effect of increased micelle size (micelle aggregates) and decreased hydrophobic content. When conjugated with larger generation dendrimers, the micelle core growth of the $B_{16}E_{42}$−dendrimer conjugates is more or less restricted by repulsion within the dendrimer periphery; i.e., each micelle of $B_{16}E_{42}$−G3a has an effective B block of 112 on average compared to those of $B_{16}E_{42}$ with 177 B blocks per micelle core. Although with an equal or even smaller hydrophobic core, the $B_{16}E_{42}$−dendrimer conjugates showed enhanced solubilization capacities compared to $B_{16}E_{42}$. Assuming that the solubilization capacity is proportional to the core volume and that the efficiencies of drug molecules penetrating into the micelle cores of the block copolymers and into those of the dendrimer conjugates are equal, it is concluded that reduced solubilization in the smaller micelle cores is more than compensated by the incorporation of drug molecules within the micelle coronas or between the cavities of micelle aggregates.

Conclusions

The synthesis and characterization of the conjugates of BE copolymers and PAMAM dendrimers of different generations are reported. Light scattering studies indicated that the amphiphilic conjugates are able to self-associate in aqueous buffer solution and form spherical "flowerlike" micelles which are composed of a hydrophobic oxybutylene core and dendrimer periphery. Further aggregation of spherical micelles was found in the solutions of conjugates with long polymer chains and small dendrimer molecules, which is attributed to the reduced steric or electrostatic repulsion and the small proportion of molecules with multiple BE chains. In a study of the solubilization of poorly water-soluble drugs in micellar solutions of the BE−dendrimer conjugates, it was shown that the solubilizing abilities of PAMAM dendrimers were considerably improved by conjugating with BE copolymers and forming micelles. The micelle core provides a dominant locus for incorporation of hydrophobic drugs, and in addition, drug molecules are able to be encapsulated in the cavities between the poly(ethylene oxide) or dendrimer branches. Solubility enhancement of a partially ionized drug carbamazepine was less pronounced due to the low partition coefficient for this drug in the micelle core. The findings of this work suggest a potential new approach to the development of drug carriers in formulation design.

Acknowledgment. We thank Dr. Colin Booth, Dr. Yang Zhuo, and Dr. Frank Heatley for assistance with copolymer synthesis and characterization and AstraZeneca for financial support.

References and Notes

(1) Tomalia, D. A.; Baker, H.; Dewald, J.; Hall, M.; Kallos, G.; Martin, S.; Roeck, J.; Ryder, J.; Smith, P. *Polym. J.* **1985**, *17*, 117–132.
(2) Tomalia, D. A.; Naylor, A. M.; Goddard, W. A.III *Angew. Chem., Int. Ed.* **1990**, *29*, 138–175.
(3) Esfand, R.; Tomalia, D. A. *Drug Discovery Today* **2001**, *6*, 427–436.
(4) D'Emanuele, A.; Attwood, D.; Abu-Rmaileh, R. In *Encyclopedia of Pharmaceutucal Technology*, 2nd ed.; Swarbrick, J., Boylan, J. C., Eds.; Marcel Dekker: New York, 2003; pp 1−21.
(5) D'Emanuele, A.; Attwood, D. *Adv. Drug Delivery Rev.* **2005**, *57*, 2147–2162.
(6) Majoros, I. J.; Williams, C. R.; Baker, J. R.Jr. *Curr. Top. Med. Chem.* **2008**, *8*, 1165–1179.
(7) Jevprasesphant, R.; Penny, J.; Attwood, D.; D'Emanuele, A. *J. Controlled Release* **2004**, *97*, 259–267.
(8) Najlah, M.; Freeman, S.; Attwood, D.; D'Emanuele, A. *Int. J. Pharm.* **2006**, *308*, 175–182.
(9) Milhem, O. M.; Myles, C.; McKeown, N. B.; Attwood, D.; D'Emanuele, A. *Int. J. Pharm.* **2000**, *197*, 239–241.
(10) Chauhan, A. S.; Sridevi, S.; Chalasani, K. B.; Jain, A. K.; Jain, S. K.; Jain, N. K.; Diwan, P. V. *J. Controlled Release* **2003**, *90*, 335–343.
(11) Beezer, A. E.; King, A. S. H.; Martin, I. K.; Mitchel, J. C.; Twyman, L. J.; Wain, C. F. *Tetrahedron* **2003**, *59*, 3873–3880.
(12) Cheng, Y.; Xu, T. *Eur. J. Med. Chem.* **2005**, *40*, 1384–1389.
(13) Kojima, C.; Kono, K.; Maruyama, K.; Takagishi, T. *Bioconjugate Chem.* **2000**, *11*, 910–917.
(14) Pan, G.; Lemmouchi, Y.; Akala, E. O.; Bakare, O. *J. Bioact. Compat. Polym.* **2005**, *20*, 113–128.
(15) Yang, H.; Morris, J. J.; Lopina, S. T. *J. Colloid Interface Sci.* **2004**, *273*, 148–154.
(16) (a) Gitsov, I.; Fréchet, J. M. J. *Macromolecules* **1993**, *26*, 6536–6546. (b) Gitsov, I. *J. Polym. Sci., Part A: Polym. Chem.* **2008**, *46*, 5295–5314. (c) Gitsov, I.; Simonyan, A.; Vladimirov, N. G. *J. Polym. Sci., Part A: Polym. Chem.* **2007**, *45*, 5136–5148.
(17) (a) Fréchet, J. M. J.; Gitsov, I.; Monteil, T.; Rochat, S.; Sassi, J. F.; Vergelati, C.; Yu, D. *Chem. Mater.* **1999**, *11*, 1267–1274. (b) Fréchet, J. M. J.; Gitsov, I. *Macromol. Symp.* **1995**, *98*, 441–465.
(18) (a) Gitsov, I.; Lambrych, K. R.; Remnant, V. A.; Pracitto, R. *J. Polym. Sci., Part A: Polym. Chem.* **2000**, *38*, 2711–2727. (b) Simonyan, A.; Gitsov, I. *Langmuir* **2008**, *24*, 11431–11441.

(19) Chapman, T. M.; Hillyer, G. L.; Mahan, E. J.; Shaffer, K. A. *J. Am. Chem. Soc.* **1994**, *116*, 11195–11196.
(20) (a) Chang, Y.; Kwon, Y. C.; Lee, S. C.; Kim, C. *Macromolecules* **2000**, *33*, 4496–4500. (b) Chang, Y.; Kim, C. *J. Polym. Sci., Part A: Polym. Chem.* **2001**, *39*, 918–926.
(21) (a) Namazi, H.; Adeli, M. *J. Polym. Sci., Part A: Polym. Chem.* **2005**, *43*, 28–41. (b) Namazi, H.; Adeli, M. *Polymer* **2005**, *46*, 10788–10799.
(22) Kim, T. I.; Seo, H. J.; Choi, J. S.; Jang, H. S.; Baek, J.; Kim, K.; Park, J. S. *Biomacromolecules* **2004**, *5*, 2487–2492.
(23) Nguyen, P. M.; Hammond, P. T. *Langmuir* **2006**, *22*, 7825–7832.
(24) Booth, C.; Attwood, D. *Macromol. Rapid Commun.* **2000**, *21*, 501–527.
(25) Booth, C.; Attwood, D.; Price, C. *Phys. Chem. Chem. Phys.* **2006**, *8*, 3612–3622.
(26) (a) Alexandridis, P.; Athanassiou, V.; Hatton, T. A. *Langmuir* **1995**, *11*, 2442–2450. (b) Goldmints, I.; Yu, G.-E.; Booth, C.; Smith, K. A.; Hatton, T. A. *Langmuir* **1999**, *15*, 1651–1656.
(27) Crothers, M.; Zhou, Z.; Ricardo, N. M. P. S.; Yang, Z.; Taboada, P.; Chaibundit, C.; Attwood, D.; Booth, C. *Int. J. Pharm.* **2005**, *293*, 91–100.
(28) Attwood, D.; Zhou, Z.; Booth, C. *Expert Opin. Drug Delivery* **2007**, *4*, 533–546.
(29) Zhou, Z.; Chaibundit, C.; D'Emanuele, A.; Lennon, K.; Attwood, D.; Booth, C. *Int. J. Pharm.* **2008**, *354*, 82–87.
(30) Yang, Z.; Pickard, S.; Deng, N. J.; Barlow, R. J.; Attwood, D.; Booth, C. *Macromolecules* **1994**, *27*, 2371–2379.
(31) Heatley, F.; Yu, G.-E.; Sun, W. B.; Pywell, E. J.; Mobbs, R. H.; Booth, C. *Eur. Polym. J.* **1990**, *26*, 583–592.
(32) Yu, G.-E.; Ameri, M.; Yang, Z.; Attwood, D.; Price, C.; Booth, C. *J. Phys. Chem. B* **1997**, *101*, 4394–4401.
(33) Shi, X. Y.; Banyai, I.; Islam, M. T.; Lesniak, W.; Davis, D. Z.; Baker, J. R.; Balogh, L. P. *Polymer* **2005**, *46*, 3022–3034.
(34) Provencher, S. *Makromol. Chem.* **1979**, *180*, 201–209.
(35) Carnahan, N. F.; Starling, K. E. *J. Chem. Phys.* **1969**, *51*, 635–636.
(36) Yang, Y. W.; Yang, Z.; Zhou, Z. K.; Attwood, D.; Booth, C. *Macromolecules* **1996**, *29*, 670–680.
(37) Liu, T. B.; Zhou, Z. K.; Wu, C. H.; Nace, V. M.; Chu, B. *J. Phys. Chem. B* **1998**, *102*, 2875–2882.
(38) Castelletto, V.; Hamley, I. W.; Yuan, X. F.; Kelarakis, A.; Booth, C. *Soft Matter* **2005**, *1*, 138–145.
(39) Mai, S. M.; Booth, C.; Nace, V. M. *Eur. Polym. J.* **1997**, *33*, 991–996.
(40) Flory, P. J. *Statistical Mechanics of Chain Molecules*; Interscience: New York, 1969.